Orbital Magnetism in Transition-Metal Clusters: From Hund's Rules to Bulk Quenching

R. A. Guirado-López,[1] J. Dorantes-Dávila,[1,2] and G. M. Pastor[2]

[1]*Instituto de Física, Universidad Autónoma de San Luis Potosí, San Luis Potosí, Mexico*

[2]*Laboratoire de Physique Quantique, Centre National de la Recherche Scientifique, Université Paul Sabatier, Toulouse, France*

(Received 28 February 2000; revised manuscript received 18 November 2002; published 5 June 2003)

The local and average orbital moments $\langle L\rangle$ of transition-metal (TM) clusters are determined bridging the gap between atomic Hund's rules and solid-state quenching. A remarkable enhancement of $\langle L\rangle$ is revealed in agreement with recent measurements. In small Ni_N ($N \leq 10$), $\langle L\rangle$ represents (20–40)% of the total magnetization and is therefore crucial for the comparison between theory and experiment. Larger clusters ($N \geq 150$) show nearly bulklike quenching at the interior but retain a considerable surface enhancement. Trends for different TM's are discussed.

DOI: 10.1103/PhysRevLett.90.226402 PACS numbers: 71.70.Ej, 36.40.Cg, 75.10.Lp, 75.75.+a

In atoms, Hund's rules predict maximum orbital angular moment L compatible with maximum spin multiplicity, while in transition-metal (TM) solids, electron delocalization and band formation result in an almost complete quenching of $\langle L\rangle$. Such intrinsic differences between atomic and bulk behaviors are characteristic of systems developing itinerant-electron magnetism. Consequently, investigations of orbital magnetism in TM clusters—in the way from the atom to the solid—should reveal novel size-dependent phenomena that are important both from a fundamental standpoint and in view of applications of cluster-based magnetic nanostructures. These general considerations already indicate that $\langle L\rangle$ should be very sensitive to the local environment of the atoms. Indeed, recent experiments on chains [1] and clusters at surfaces [2–4] show that $\langle L\rangle$ is typically a factor of 2–5 larger than in the corresponding solids. Electronic calculations on small supported clusters confirm these conclusions [5]. In the case of free clusters, however, very little is known about this problem, particularly from the point of view of theory which has been so far concerned only with the spin contributions [6,7]. This is quite remarkable since a size-dependent enhancement of $\langle L\rangle$ would have direct consequences on the average magnetic moments per atom and for the comparison with experiment [8,9]. The purpose of this Letter is to present a systematic theoretical investigation of orbital magnetism in free TM clusters including the crossover from the atom to the bulk.

The theoretical framework [10] is given by the electronic Hamiltonian $H = H_0 + H_C + H_{SO}$. The interatomic hopping term H_0 describes the single-particle electronic structure of the cluster in a tight-binding approximation by including either the d electrons alone, or the s, p, and d valence electrons. The Coulomb-interaction term in the unrestricted Hartree-Fock approximation is $H_C = \sum_{im\sigma} \Delta\varepsilon_{im\sigma} \hat{n}_{im\sigma}$, where

$$\Delta\varepsilon_{im\sigma} = \sum_{m'} \left(U_{mm'} - \frac{J_{mm'}}{2} \right) \nu_{im'} - \frac{\sigma}{2} \sum_{m'} J_{mm'} \mu_{im'} \quad (1)$$

takes into account the effects of redistributions of the spin- and orbital-polarized density $\langle \hat{n}_{im\sigma}\rangle$. The direct (exchange) integrals are denoted by $U_{mm'}$ ($J_{mm'}$). The average occupation and spin polarization of orbital im are $\nu_{im} = \langle \hat{n}_{im\uparrow}\rangle + \langle \hat{n}_{im\downarrow}\rangle$ and $\mu_{im} = \langle \hat{n}_{im\uparrow}\rangle - \langle \hat{n}_{im\downarrow}\rangle$. Finally, H_{SO} treats spin-orbit (SO) interactions in the usual intra-atomic approximation [10,11].

The local densities of electronic states (DOS) $\rho^{\delta}_{im\sigma}(\varepsilon)$ are determined self-consistently for each orientation δ of the spin magnetization $\vec{S}$. We consider $\delta = z$, usually along a principal C_n symmetry axis of the cluster, and one or more directions within the xy plane. The associated single-particle problem is solved by using Haydock-Heine-Kelly's recursion method with a controlled accuracy [6,10]. Finally, the local orbital moments $L_\delta(i)$ at different atoms i are determined from

$$L_\delta(i) = \sum_{\sigma} \sum_{m=-2}^{2} \int_{-\infty}^{\varepsilon_F} m \rho^{\delta}_{im\sigma}(\varepsilon) d\varepsilon, \quad (2)$$

where m refers to the magnetic quantum number [12].

The parameters used in the calculations are specified as follows. The two-center d-electron hopping integrals are given by the canonical expression in terms of the corresponding bulk d-band width. The intra-atomic Coulomb integrals $U_{mm'}$ and $J_{mm'}$ are expressed in terms of the three independent radial Coulomb integrals $F^{(0)}$, $F^{(2)}$, and $F^{(4)}$ allowed by atomic symmetry [13]. These are chosen by taking the ratios $F^{(0)}/F^{(2)}$ and $F^{(4)}/F^{(2)}$ from atomic calculations and by fitting $F^{(2)}$ to reproduce the bulk spin moment [$\overline{U}_{mm'} = F^{(0)} = 9.5$ eV and $\overline{J}_{mm'} = (F^{(2)} + F^{(4)})/14 = 0.51$ eV for Ni]. As discussed below, our main results and conclusions are not qualitatively affected by the absolute values of the Coulomb integrals, as given by $\overline{U}_{mm'}$, or by the orbital dependence of $U_{mm'}$ and $J_{mm'}$. The SO coupling constants are taken from Ref. [11] ($\xi = 110$ meV for Ni). The role of sp electrons and spd hybridizations is investigated by varying the d-band filling n_d around the bulk values ($n_d = 7$, 8, and 9 for Fe, Co, and Ni, respectively) and by performing

 © 2003 The American Physical Society

self-consistent *spd*-band calculations for representative examples. A first test on the accuracy of the model and parameter choice is provided by our bulk results: $L_b(\mathrm{Fe}) = 0.094\mu_B$, $L_b(\mathrm{Co}) = 0.131\mu_B$, and $L_b(\mathrm{Ni}) = 0.056\mu_B$, which agree with the experimental values $L_b(\mathrm{Fe}) = 0.092\mu_B$, $L_b(\mathrm{Co}) = 0.147\mu_B$, and $L_b(\mathrm{Ni}) = 0.051\mu_B$. For atoms all Hund's rules are followed [13].

In order to investigate the crossover from atomic L to bulklike quenching of $\langle L\rangle$ with increasing cluster size we focus on Ni_N clusters. Besides its experimental relevance [8,9], Ni is very interesting, since the difference between the atomic orbital moment L_a and bulk moment L_b is dramatic ($L_a = 2\mu_B$ for s^1d^9, and $L_b = 0.05\mu_B$). Moreover, the spin moments in Ni_N are the smallest among the ferromagnetic TM's, and therefore the contribution of $\langle L\rangle$ to the magnetic moment $\langle\vec{M}\rangle = 2\langle\vec{S}\rangle + \langle\vec{L}\rangle$ should be particularly significant. In Fig. 1 results are given for the average orbital moment per atom $\langle L_\delta\rangle = [\sum_{i=1}^{N} L_\delta(i)]/N$ of Ni_N with $N \leq 165$, having face-centered-cubic (fcc) or icosahedral-like geometries. Low-symmetry structures and two-dimensional (2D) islands are also considered. These are representative of different local symmetries and shapes and allow one to quantify the role of cluster structure on orbital magnetism. On the one hand, we observe that the reduction of system size causes a remarkable enhancement of $\langle L_\delta\rangle$ with respect to the solid. Values about 6–8 times larger than L_b are not uncommon. On the other hand, comparison with the atomic result L_a shows that the largest part of the quenching of L takes place already at the smallest clusters, as soon as full rotational symmetry is lost. For example, for Ni_3 we obtain $\langle L_z\rangle = 0.47\mu_B$, and for Ni_4 $\langle L_z\rangle = 0.35\mu_B$. Concerning the size dependence, one observes that $\langle L_\delta\rangle$ decreases with increasing N showing some oscillations as bulklike quenching is approached (see Fig. 1). Notice that an important enhancement of $\langle L_\delta\rangle$, about 100%, is still present even for the largest considered sizes (e.g., $\langle L_\delta\rangle/L_b = 1.8$ for $N = 165$). In smaller clusters, $\langle L_\delta\rangle/L_b$ ranges from $\langle L_\delta\rangle/L_b \simeq 3$ for $N = 50$–80, to $\langle L_\delta\rangle/L_b \simeq 5$ for $N = 10$–20. One concludes that orbital magnetism is the source of an important contribution to the size-dependent magnetic properties of Ni clusters.

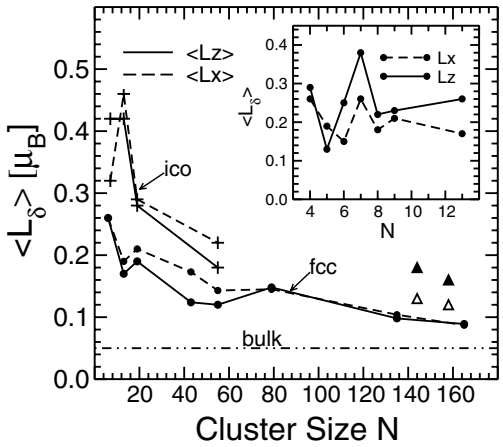

FIG. 1. Average orbital magnetic moment per atom $\langle L_\delta\rangle$ of Ni_N clusters with fcc-like (dots) and icosahedral-like structures (crosses). The magnetization direction δ is a principal C_n symmetry axis ($\delta = z$) or a NN bond perpendicular to z ($\delta = x$). Full (open) triangles refer to coinlike bilayer clusters with perpendicular (in-plane) magnetization. Results for small clusters are given in the inset.

In Fig. 1 results are also given for icosahedral clusters having $N \leq 55$ atoms. $\langle L_\delta\rangle$ decreases with increasing N in a similar way as for the fcc geometries. Nevertheless, the fivefold symmetric structures yield in general significantly larger $\langle L_\delta\rangle$ than the cubic-symmetric ones. Notice that the results for $N \geq 13$ concern mainly highly symmetric structures with nearly spherical shape and closed nearest neighbor (NN) shells. Clusters with lower symmetry usually present a very rich size dependence, particularly when the proportion of surface atoms is large. This is illustrated by the results for $N \leq 13$ given in the inset. Here, we consider the optimized geometries derived from *ab initio* calculations, which have low symmetry and significant bond-length contractions [7]. Structural changes may also affect the convergence to bulklike quenching for large N, particularly for clusters on surfaces, which shape can be experimentally tuned at least to some extent [1–4]. To investigate this problem we performed calculations for two-layer-thick coinlike Ni_N, which are indicated by the triangles in Fig. 1 ($N = 144$ and 158). For these 2D islands, $\langle L_\delta\rangle$ is much larger than for 3D fcc clusters of comparable size. The enhancement with respect to L_b is here about a factor of 3. Similar trends are found for other TM's, in qualitative agreement with recent experiments on Fe and Co particles [1–4].

From the solid-state perspective, the enhancement of $\langle L_\delta\rangle$ can be qualitatively understood as the result of the following major contributions that are related to the changes in the local environment of the atoms. First, the reduction of local coordination number with decreasing N causes an increase of the local spin polarizations $S_\delta(i)$ which induces larger orbital moments by means of the SO interactions. Second, the orbital dependence of intra-atomic Coulomb interaction favors the occupation of high-m states thereby amplifying the enhancement of $\langle L_\delta\rangle$. Although this contribution is quantitatively important, typically (30–40)% of the value of $\langle L_\delta\rangle$, it does affect significantly the trends as a function of size and structure. Third, the presence of degeneracies in the single-particle spectrum allows a more effective SO mixing that enhances $L_\delta(i)$ even in situations where $S_\delta(i)$ is saturated. Qualitatively, the size-dependent magnetic moments are determined by the competition between the kinetic energy, which favors electron delocalization and small moments, and the Coulomb interactions, which tend to suppress charge fluctuations and lead to Hund rules.

Thus, low-spin and quenched-L states become comparatively less stable than high-spin and enhanced-L states as N is reduced. Notice, moreover, that the changes in $S_\delta(i)$ and $L_\delta(i)$ involve different energy scales. Therefore, the occupations of the different m orbitals may vary without altering the spin polarizations (e.g., compare icosahedral and fcc clusters in Fig. 1). Finally, one also observes less predictable effects related to the details of the electronic structure and its dependence on cluster geometry, such as the presence of high-symmetry axes or changes in bond length.

The environment dependence of the local orbital moments $L_\delta(i)$ provides further insight on the enhancement of $\langle L_\delta \rangle$ in small clusters, and on the development of bulklike quenching for large N. Figure 2 displays $L_\delta(i)$ in fcc Ni clusters formed by a central atom ($i = 1$) and the successive shells of its NN's. One observes that $L_\delta(i)$ generally increases with i, showing some oscillations as we move from the center to the surface of the cluster. Therefore, the enhancement of $\langle L_\delta \rangle$ is driven by the surface, as is the case for the spin moments [6]. A similar behavior is found for icosahedral geometries. For small N (e.g., $N = 19$ and 55) the enhancement of $L_\delta(i)$ concerns practically all atoms, including those with a complete NN shell. For larger sizes ($N \geq 135$) bulklike quenching starts to set in at the interior of the cluster, leaving significantly enhanced orbital moments only at a few outermost shells. As expected, one approaches the behavior found for TM surfaces, where the enhanced $L_\delta(i)$ are restricted to a few uppermost layers. A droplet model, i.e., $(\langle L_\delta \rangle - L_b) \propto N^{-1/3}$, is in fact a good first approximation for $N \geq 150$–200, although the convergence to L_b remains rather slow. The fact that $L_\delta(i) \simeq L_b$ for inner atoms indicates that cubic point-group symmetry, absent in all atoms except the central one, is not essential for reaching nearly bulklike quenching. Instead, the recovery of a bulklike local atomic environment seems a more appropriate interpretation.

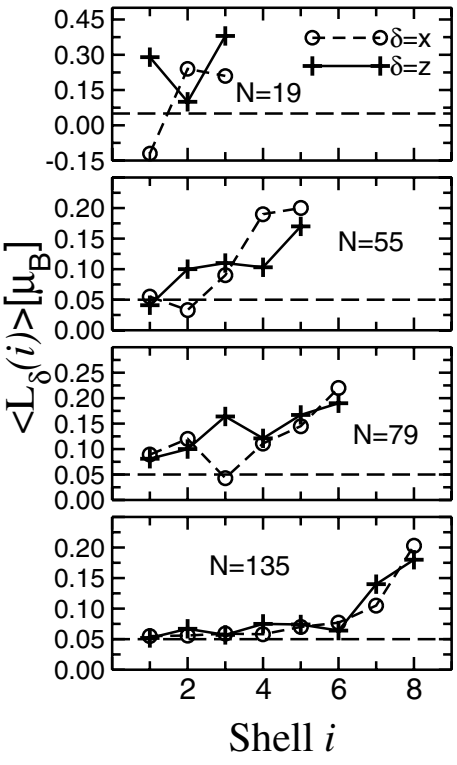

FIG. 2. Local orbital moments along the spin magnetization direction δ in fcc-like Ni_N clusters averaged at each NN shell i surrounding the central atom $i = 1$.

Figure 2 shows that the anisotropy of the local moments $\Delta L(i) = L_z(i) - L_x(i)$ increases with decreasing N and depends strongly on the local environment. Since $\Delta L(i)$ often changes sign as a function of i, the magnetization direction δ yielding the largest *local* orbital moment does not necessarily correspond to the easy-magnetization axis of the cluster. The cancellation of contributions from different i results in a relatively small anisotropy of the average per atom $\langle L_\delta \rangle$ (see Fig. 1) and is consistent with the small magnetic anisotropy energies found in large cubic-symmetric clusters [14].

In past years, the spin magnetic moments of small Ni_N clusters have been studied systematically by using density-functional theory [7] and comparing the results with the average magnetizations per atom $\bar{\mu}_N$ derived from Stern-Gerlach experiments [9]. Despite some quantitative differences among the various calculations, they all agree that the theoretical ground-state spin moments are systematically smaller than the experimental $\bar{\mu}_N$, by about $(0.3$–$0.6)\mu_B$ for $N \leq 13$. In this work we have determined for the first time the orbital moments in Ni_N corresponding to the structures reported in Ref. [7]. As shown in the inset of Fig. 1, one obtains $\langle L_\delta \rangle \simeq (0.2$–$0.4)\mu_B$ for $N \leq 13$. Therefore, $\langle L_\delta \rangle$ is an important contribution to the cluster magnetization (20–40%). In fact, taking into account the enhanced orbital moments, which in Ni align parallel to the spin moments, removes the largest part of the discrepancy between theory and experiment, thereby resolving the previous controversy on this subject. The remaining differences, about $(0.1$–$0.2)\mu_B$, are not far from the estimated experimental uncertainties. This could also be related to correlation effects, which should favor electron localization leading to more atomiclike orbital moments and possibly to a further enhancement of $\langle L_\delta \rangle$.

The trends for other TM's and the effect of sp-d charge transfers can be inferred from Fig. 3, where $\langle L_\delta \rangle$ of a pentagonal bipyramid is given as a function of d-band filling n_d. $\langle L_\delta \rangle$ increases approximately linearly with an increasing number of d holes, as we move from Ni ($n_d \simeq 9$) to Fe ($n_d \simeq 7$). Notice that the orbital moment per d hole $\langle L_\delta \rangle / (10 - n_d) \simeq (0.25$–$0.3)\mu_B$ is quite close to recent experimental results on Fe_N clusters ($N \leq 9$) deposited on Ni/Cu(001) [4]. In addition one observes oscillations and changes of sign of the anisotropy $\Delta L =$

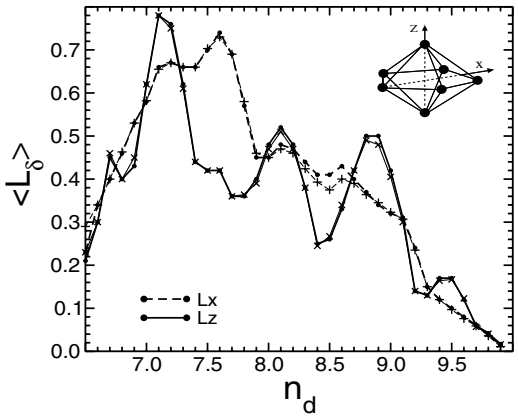

FIG. 3. Average orbital moment per atom $\langle L_\delta \rangle$ in a seven-atom TM cluster as a function of d-band filling n_d. The structure and magnetization directions δ are illustrated. Dots (crosses) refer to results using $F^{(0)} = 9.5$ eV ($F^{(0)} = 2.5$ eV).

$L_z - L_x$, which are associated to changes in the occupations of molecular states k with different orbital moments $\langle l \rangle_k$. This is consistent with previously observed oscillations of the magnetic anisotropy energy as a function of n_d [14]. One concludes that the size-dependent enhancement of $\langle L_\delta \rangle$ is important for all magnetic TM clusters.

Figure 3 shows that $\langle L_\delta \rangle$ depends very weakly on the average value of the Coulomb repulsion integrals $\overline{U}_{mm'} = F^{(0)}$. Indeed, the results for an atomiclike value $F^{(0)} = 9.5$ eV, yielding $U_{mm'} \simeq (9\text{–}10)$ eV, are almost the same as for $F^{(0)} = 2.5$ eV, yielding $U_{mm'} \simeq (2\text{–}3)$ eV, as often used in solid-state applications (see Fig. 3). This is important since a possible size dependence of the effective Coulomb-repulsion strength cannot be excluded *a priori*. The weak dependence of $\langle L_\delta \rangle$ on $F^{(0)}$ can be understood by recalling that, from a mean-field perspective, $F^{(0)}$ controls mainly the charge transfer between atoms with different local environments but has little effect on the relative occupations of the spin orbitals [see Eq. (1)]. Still, $\langle L_\delta \rangle$ is sensitive to the orbital dependence of $U_{mm'}$ and $J_{mm'}$, although the main trends as a function of size and structure are well captured already by the m-independent model. In addition, spd-band calculations have been performed showing that sp-d hybridizations do not affect strongly the calculated $\langle L_\delta \rangle$ [typically by only (10–15)%]. These results confirm the general validity of our conclusions.

Finally, the properties of Rh clusters deserve to be briefly mentioned, since here the spin moments are smaller and the SO couplings stronger than in $3d$ TM's. Our calculations show that the orbital contributions to the total magnetic moment are also significant in Rh_N. If bulklike NN distances are assumed, we obtain $\langle L_\delta \rangle = (0.1\text{–}0.25)\mu_B$ for $N \leq 19$, which is similar to what is found in Ni_N. Relaxed Rh_N geometries present considerable bond-length contractions that tend to reduce $\langle L_\delta \rangle = (0.1\text{–}0.18)\mu_B$ ($N \leq 19$). This still represents about (15–25)% of the total magnetic moment. Larger Rh_N clusters show a particularly strong size and structural dependence of $\langle L_\delta \rangle$ due to the rapid decrease of the spin magnetization with increasing N.

In conclusion, a systematic self-consistent study of orbital magnetism in TM clusters has been performed which revealed remarkable properties of L as a function of size, geometry, and composition including the crossover from atomic to bulklike behavior. The importance of orbital contributions to the magnetic moments has been demonstrated, particularly concerning the comparison between theory and experiment. Among the future implications of this work, it would be relevant to investigate the role of electron correlations beyond the present mean-field theory, since they may affect the localized versus delocalized characters of the d-electron states.

This work was supported by EU GROWTH project AMMARE (Contract No. G5RD-CT-2001-00478), by CONACyT Mexico (Grant No. 39517), and by IMP Mexico (Grant No. FIES-98-101-I). Computer resources were provided by IDRIS (France).

[1] P. Gambardella *et al.*, Nature (London) **416**, 301 (2002).
[2] C. Binns, Surf. Sci. Rep. **44**, 1 (2001).
[3] T. Koide *et al.*, Phys. Rev. Lett. **87**, 257201 (2001).
[4] J.T. Lau *et al.*, Phys. Rev. Lett. **89**, 057201 (2002).
[5] B. Nonas *et al.*, Phys. Rev. Lett. **86**, 2146 (2001); B. Lazarovits *et al.*, Phys. Rev. B **65**, 104441 (2002); R. Félix-Medina *et al.*, Phys. Rev. B **67**, 094430 (2003).
[6] See, e.g., G.M. Pastor, in *Atomic Clusters and Nanoparticles*, edited by C. Guet *et al.* (Springer, Berlin, 2001), p. 335.
[7] M. Castro *et al.*, Chem. Phys. Lett. **271**, 133 (1997); B.V. Reddy *et al.*, J. Phys. Chem. A **102**, 1748 (1998).
[8] I. M. L. Billas *et al.*, Science **265**, 1662 (1994).
[9] S. E. Apsel *et al.*, Phys. Rev. Lett. **76**, 1441 (1996); M. B. Knickelbein, J. Chem. Phys. **115**, 1983 (2001).
[10] J. Dorantes-Dávila and G. M. Pastor, Phys. Rev. Lett. **81**, 208 (1998).
[11] P. Bruno, *Magnetismus von Festkörpern und Grenzflächen* (KFA, Jülich, 1993), Chap. 24.
[12] $\vec{L} = \sum_\sigma \int d\vec{r} \hat{\Psi}^\dagger_\sigma(\vec{r}) \vec{r} \times \vec{p} \hat{\Psi}_\sigma(\vec{r})$, where $\hat{\Psi}_\sigma(\vec{r}) = \sum_{im} \psi_{im}(\vec{r}) \hat{c}_{im\sigma}$ is expanded in a d-orbital basis $\psi_{im}(\vec{r})$ centered at each atom i. Neglecting the overlaps between the ψ_{im} on different atoms, one obtains $\hat{L}_\delta = \sum_i \hat{l}_{i\delta} = \sum_{im\sigma} m \hat{c}^\dagger_{im\sigma} \hat{c}_{im\sigma}$. Thus, $L_\delta(i) = \langle \hat{l}_{i\delta} \rangle = \sum_{m\sigma} m \langle \hat{n}_{im\sigma} \rangle$.
[13] J. C. Slater, *Quantum Theory of Atomic Structure* (McGraw-Hill, New York, 1960), Vol. I.
[14] G. M. Pastor *et al.*, Phys. Rev. Lett. **75**, 326 (1995).